

Available online at www.sciencedirect.com**ScienceDirect**

Procedia Earth and Planetary Science 17 (2017) 344 – 347

Procedia
Earth and Planetary Science

15th Water-Rock Interaction International Symposium, WRI-15

Unraveling the formation of large amounts of calcite scaling in geothermal wells in the Bavarian Molasse Basin: a reactive transport modeling approach

Christoph Wanner^{a,1}, Florian Eichinger^b, Thomas Jahrfeld^c, Larryn W. Diamond^a^a*Rock-Water Interaction Group, Institute of Geological Sciences, University of Bern, Baltzerstrasse 1+3, CH-3012 Bern, Switzerland*^b*Hydroisotop GmbH, Woelkestr. 9, D-85301 Schweitenkirchen, Germany*^c*renerco plan consult, Herzog-Heinrich Str. 13, D-80336 München, Germany*

Abstract

Results from reactive transport simulations performed for the geothermal plant in Kirchstockach, located in the Bavarian Molasse Basin in southern Germany, are presented to unravel the formation of calcite scaling. Simulation results successfully predict the calcite scaling profile observed along the production well if supersaturation with respect to calcite is specified for the model water leaving the pump at 800 m depth. This observation is in good agreement with a previous study suggesting that gas exsolution (i.e., boiling) occurring at the pump due to an unwanted pressure drop is the most likely driver for the formation of those calcite scalings.

© 2017 The Authors. Published by Elsevier B.V. This is an open access article under the CC BY-NC-ND license (<http://creativecommons.org/licenses/by-nc-nd/4.0/>).

Peer-review under responsibility of the organizing committee of WRI-15

Keywords: Scaling; calcite; geothermal energy; reactive transport; boiling

1. Introduction

The carbonate-dominated Malm aquifer in the Bavarian Molasse Basin in southern Germany is being widely exploited and explored for geothermal energy¹⁻³. Owing to karstification, the fracture spacing and permeability is high enough for continuous water extraction. Therefore, some 40 wells have been drilled in the greater Munich area over the last 10 years. Typical flow rates are between 30 and 130 L s⁻¹ and the production temperatures reach up to 150 °C. Despite these favorable reservoir conditions, the use of many of the wells for heat and power production is

* Corresponding author. Tel.: +41316314023; fax: +41316314843.

E-mail address: wanner@geo.unibe.ch

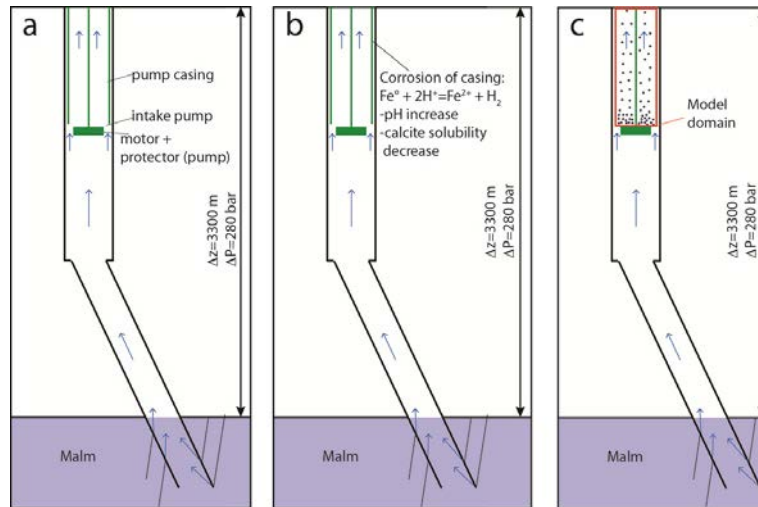


Fig. 1. Scenarios of the formation of calcite scaling: (a) linear decompression scenario in which calcite precipitation occurs only due to the solubility decrease associated with the linear pressure decrease of ca. 280 bar as the thermal water is pumped from the Malm aquifer to the surface. (b) Corrosion scenario in which calcite precipitation is induced by corrosion of the casing and the associated pH increase and calcite solubility decrease. (c) Boiling scenario in which calcite precipitation is caused by gas exsolution from the produced thermal water due to a localized pressure drop, most likely located within the centrifugal pump. Scenario c also shows the section of the well for which reactive transport model simulations were performed.

highly challenging. The main difficulty, especially in the deep (>3000 m) boreholes with temperatures >120 °C, is that substantial amounts of calcite-dominated scaling are hindering the proper operation of the pumps within the wells and of the heat exchangers at the surface. In a previous study⁴ we presented an extensive dataset from the geothermal plant in Kirchstockach, which was collected during the production period between December 2014 and March 2015. Based on chemical analyses of wellhead water samples, chemical and mineralogical analyses of scaling collected along the uppermost 800 m of the production well, and gas analyses of fluid inclusions identified in calcite crystals we postulated three scenarios that can explain the formation of the calcite scaling (Fig. 1). The scenarios were evaluated by performing geochemical speciation calculations taking into account the pressure dependence of calcite solubility. The calculations suggested that the boiling scenario, where gas exsolves at the pump due to an unwanted pressure drop, is the most likely driver for scale formation⁴. For this contribution we present results from reactive transport model simulations performed for the three scenarios to further test the three scale formation scenarios.

2. Model setup

Reactive transport model simulations were performed for each scaling scenario (Fig. 1) using the code TOUGHREACT V3⁵. Simulations were run for the section of the production well located above the pump. Since the pump was situated at a depth of 800 m during the studied production period, the vertical extent of the model is 800 m (Fig. 2a). The temperature was kept constant at 135 °C, corresponding to the long-term average wellhead temperature. At the upstream model boundary the pressure was fixed to 18 bar, corresponding to the pressure under which the geothermal plant is being operated at the surface. Within the well a hydrostatic pressure distribution was defined yielding a pressure of about 90 bar at the downstream model boundary. To be able to simulate that scaling formation only occurs at the surface of the casing a 2D radial mesh was defined (Fig. 2b). In doing so, the production well was discretized into 7 radially concentric grid cylinders. The radial discretization further allowed the definition of a parabolic velocity distribution $v(r)$ across the well according to the Poiseuille equation:

$$v(r) = \frac{1}{4\eta} \cdot \frac{\Delta P}{\Delta z} (R^2 - r^2) \quad (1)$$

where η refers to the fluid viscosity, ΔP is the pressure drop occurring along the production well due to frictional forces, and R and r refer to the radii of the well and the location at which the velocity is calculated, respectively. The Poiseuille law was implemented by specifying a corresponding permeability distribution along the radial grid, which yielded a constant velocity profile as illustrated in Fig. 2c and a flux-averaged upflow rate of 87 L s^{-1} corresponding to the average production rate during the studied production period.

2.1. Initial and boundary conditions

The chemical fluid composition specified as initial and boundary condition depends on the simulated scenario (Table 1). For the linear decompression and corrosion scenarios (Fig. 1a,b) a fluid in equilibrium with the dolomite- and calcite-bearing Malm reservoir was specified. In contrast, for the boiling scenario (Fig. 1c) we specified a fluid composition that is supersaturated with respect to calcite and dolomite and reflects a reservoir fluid that previously experienced CO_2 degassing associated with boiling of the produced water at the pump. Moreover, the specified composition corresponds to the wellhead sample showing the maximum calcite and dolomite supersaturation during the investigated production period.

Table 1: Chemical composition specified as initial and boundary condition for the three simulation scenarios (Fig. 1). All concentrations are given in mg L^{-1} except for dissolved inorganic carbon (DIC), which is in mmol L^{-1} .

Scenario	pH	DIC	Ca^{2+}	Mg^{2+}	Na^+	Cl^-	SI calcite	SI dolomite
Linear decompression	6.41	9.5	18.9	2.0	117	75	0.0	0.0
Corrosion	6.41	9.5	18.9	2.0	117	75	0.0	0.0
Boiling	6.76	7.0	18.9	2.0	117	75	0.41	0.61

A specific geochemical reaction network was specified for each of the three scenarios (Fig. 1). For the linear decompression scenario, calcite was allowed to form in the outermost grid block (i.e., casing surface) if it became supersaturated due to the linear pressure decrease during upflow (Fig. 2a). To simulate the maximum amount of scaling, calcite precipitation was computed as an equilibrium reaction, which means that calcite was kept at saturation as in the case of a high precipitation rate. For the corrosion scenario the surface of the casing was considered to be susceptible to anaerobic iron oxidation:



A particular characteristic of the investigated well was that a segment of the casing (~45 area% of the total casing) had been coated by a thin plastic film to protect it from corrosion. Accordingly, iron corrosion (eq. (2)) was only simulated for the segments of the casing that were not coated. Similar to the linear decompression scenario, calcite was allowed to precipitate if it became supersaturated. For the boiling scenario, calcite precipitation was the only reaction occurring at the surface of the casing. In contrast to the other two scenarios calcite precipitation was simulated as a kinetic reaction taking into account the average precipitation rate derived from the amount of scaling formed over the investigated production period ($7.1 \times 10^{-13} \text{ mol L}^{-1} \text{ s}^{-1}$)⁴. To account for the observation that the scaling thickness is larger along the uncoated tubes, the rate was increased by 67% for the uncoated tubes and decreased by 67% for the coated tubes.

3. Model results and discussion

Simulated thicknesses of calcite scaling are compared with the thicknesses measured in each of the 68 casing tubes (Fig. 2d) in order to evaluate the three scaling formation scenarios (Fig. 1). The linear decompression scenario yields scales that are much thinner ($< 0.1 \text{ mm}$) than the observations. The same applies to the corrosion scenario along the coated section of the casing, because no corrosion was simulated for this interval. The minor calcite scaling in the absence of corrosion reflects the weak dependence of calcite solubility on pressure. If calcite precipitation is suppressed in the linear decompression scenario, a calcite saturation index of only 0.01 is obtained when the pressure gradually falls from 90 bar to the 18 bar plant pressure during upflow in the well (Fig. 2a).

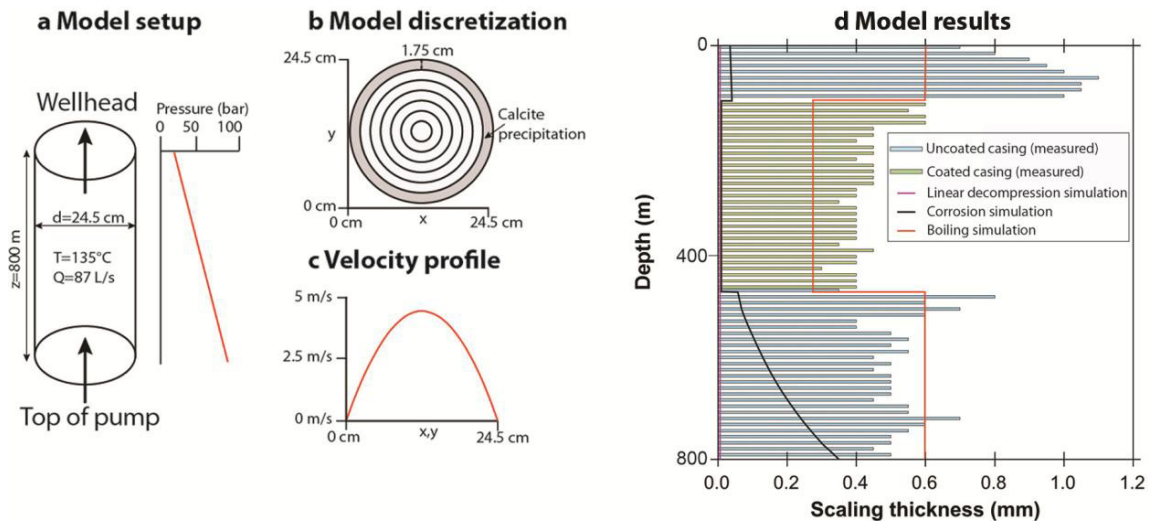


Fig. 2. Model setup, discretization, and simulation results: The section of the well above the pump was simulated at a constant temperature and at hydrostatic pressure distribution with a fixed average upflow rate of 87 L s^{-1} (a). Perpendicular to flow the model was discretized into 7 radially concentric grid blocks (i.e., cylinders) each 1.75 cm wide, whereas scaling formation was only allowed in the outermost grid block corresponding to the surface of the casing (b). The velocity profile across the well was specified according to the Poiseuille law (eq. (1)) (c). Simulation results are presented by comparing scaling thicknesses formed along the upper 800 m of the production well during the studied production period (December 2014 to March 2015) with the thicknesses simulated for the three scale formation scenarios (d). The horizontal bars correspond to the thickness measured for each of the 68 casing tubes.

For the corrosion scenario, a scaling thickness on the order of the measured thicknesses can be only obtained along the lower part of the uncoated casing section. However, this requires specification of a very high rate of anaerobic iron corrosion, such as that used to simulate highly corrosive, granular zero-valent iron⁶. The small amount of scaling predicted for the coated section as well as the need to invoke highly corrosive uncoated tubes implies that corrosion cannot be the main driver of scaling formation. Low corrosion rates are also consistent with the absence of bacteria in the produced thermal water, suggesting that corrosion is not microbially stimulated.

In contrast to the two other scenarios, the boiling scenario can reproduce the observed profile of scaling thickness nicely if the precipitation rates are specified accordingly (Fig. 2d). The main cause of the thicker scales in this scenario is the high initial supersaturation of the water entering the model at the downstream boundary (Table 1). With such a high initial supersaturation, the observed scaling thicknesses can be reproduced using plausibly slow calcite precipitation rates. We thus conclude that scaling at the Kirchstockach plant is best explained by calcite supersaturation induced at the down-hole pump. Supersaturation is most likely due to a local pressure drop caused by a high pumping rate, which in turn leads to boiling and CO_2 degassing of the produced thermal water.

References

1. Dussel M, Lüschen E, Thomas R, Agemar T, Fritzer T, Sieblitz S, Huber B, Birner J, Schulz R. Forecast for thermal water use from Upper Jurassic carbonates in the Munich region (South German Molasse Basin). *Geothermics* 2016;**60**, 13-30.
2. Lentsch D, Dorsch K, Sonnleitner N, Schubert A. Prevention of casing failures in ultra-deep geothermal wells (Germany). *Proceedings, World Geothermal Congress*, Melbourne, Australia, 19-25 April 2015.
3. Mayrhofer C, Niessner R, Baumann T. Hydrochemistry and hydrogen sulfide generating processes in the Malm aquifer, Bavarian Molasse Basin, Germany. *Hydrogeology Journal* 2014;**22**, 151-162.
4. Wanner C, Eichinger F, Jahrfield T, Diamond LW. Unraveling the formation of large amounts of calcite scalings in geothermal wells drilled into the Bavarian Molasse Basin in Southern Germany. *Geothermics* in review
5. Xu T., Sonnenthal EL, Spycher N, Zheng L. TOUGHREACT V3.0-OMP Reference Manual: A Parallel Simulation Program for Non-Isothermal Multiphase Geochemical Reactive Transport. *LBNL Manual* 2014. http://esd.lbl.gov/FILES/research/projects/tough/documentation/TOUGHREACT_V3-OMP_RefManual.pdf.
6. Jamieson-Hanes JH, Lentz AM, Amos RT, Ptacek CJ, Blowes DW. Examination of Cr(VI) treatment by zero-valent iron using in situ, real-time X-ray absorption spectroscopy and Cr isotope measurements. *Geochim. Cosmochim. Acta* 2014;**142**, 299-313.